Kinetics of Triglyceride Solubilization by Micellar Solutions of Nonionic Surfactant and Triblock Copolymer. 3. Experiments with Single Drops

P. D. Todorov,[†] G. S. Marinov,[†] P. A. Kralchevsky,*[,†] N. D. Denkov,[†] P. Durbut,[‡] G. Broze,[‡] and A. Mehreteab[§]

Laboratory of Chemical Physics & Engineering, Faculty of Chemistry, University of Sofia, 1 James Bourchier Avenue, 1164 Sofia, Bulgaria, Colgate-Palmolive R&D, Inc., Avenue du Parc Industriel, B-4041 Milmort (Herstal), Belgium, and Colgate-Palmolive Technology Center, Piscataway, New Jersey 08854-5596

Received April 15, 2002. In Final Form: July 4, 2002

We investigated the kinetics of solubilization of triglycerides (triolein and soybean oil) by observing the diminishing of individual oil drops (radius ≤ 50 μm) in a micellar surfactant solution. We used two solubilization cells. Cell no. 1 is a centimeter-sized thermostated vessel, containing the investigated micellar solution and a few oil drops. Cell no. 2 represents a set of horizontal glass capillaries filled with the solution; in each of them an oil drop was injected by a syringe. Cell no. 1 is more easy to operate, whereas cell no. 2 allows a quantitative interpretation of the results. We carried out experiments with solutions of two nonionic surfactants and investigated the effect of various additives on the solubilization rate. The addition of an anionic surfactant is found to suppress the solubilization due to an enhanced electrostatic repulsion between the micelles and the oil−water interface. This inhibitory action can be partially removed by addition of an amphoteric surfactant. Highest solubilization rates have been achieved by addition of E_n−P_m−E_n triblock copolymers (Synperonics) to the nonionic surfactant solutions. The experimental data for diminishing drops agree very well with the theoretical time dependence of the drop radius. From the fits we determined the solubilization rate, the compound kinetic constant of solubilization, and the number of oil molecules/swollen micelle, n_s. The kinetic values of n_s, determined with diminishing oil drops, are compared with the equilibrium values of n_s, independently obtained by NMR. The data confirm that, in the considered case, the time-limiting step is the adsorption of empty micelles at the oil−water interface. In particular, each swollen micelle desorbs from the triolein−water interface after taking 5−20 triolein molecules, depending on the solution's composition. The reported results can be helpful for the analysis and control of the solubilization kinetics of triglycerides and other water-insoluble oils.

1. Introduction

This is the last part in a series of three papers devoted to the solubilization of triglycerides (and other water-insoluble oils) by micellar solutions of nonionic surfactants. In the first part of this series,[1] we investigated (by NMR and static and dynamic light scattering) how the size, shape, and aggregation number of the micelles change during the solubilization of triolein in mixed aqueous solutions of the nonionic surfactant $C_{12}E_n$ ($n = 5$ or 6) and the nonionic triblock copolymer Synperonic L61 (SL61). The latter is found to strongly accelerate the solubilization, although the polymer alone is unable to solubilize triglycerides.

In the second part of this series,[2] we developed a theoretical model of oil solubilization in micellar surfactant solutions. The model describes the elementary act of solubilization as a sequence of three steps: (a) adsorption of an empty micelle at the oil−water interface; (b) uptake of oil by the empty micelle, which splits into several swollen micelles; (c) desorption of the swollen micelles. Theoretical expressions have been derived that describe the diminishing of an oil drop in the course of solubilization.

Our major goal in this article is to verify the predictions of the theoretical model from ref 2 against a set of systematic experimental data. The kinetic parameters, determined from the best fit, allow us to better understand the mechanism of solubilization and, especially, which of the aforementioned three steps is the rate-limiting one, which experimental parameter is the most appropriate characteristics of the solubilization rate, how the triblock copolymer accelerates the solubilization, how many oil molecules are taken by a swollen micelle upon its desorption from the oil−water interface, etc. In a final reckoning, the quantitative interpretation of the experimental data reveals the factors which can be used to control the solubilization kinetics of triglycerides and other water-insoluble oils.

The kinetics of solubilization can be investigated in experiments with *emulsions* which are subjected to shaking or stirring.[3,4] If the oil droplets are of submicometer size, they are involved in Brownian motion.[5,6] One way to detect solubilization in these cases is to measure the turbidity of the emulsion, which allows one

* Corresponding author. Phone: (+359) 2-962 5310. Fax: (+359) 2-962 5643. E-mail: pk@lcpe.uni-sofia.bg.
[†] University of Sofia.
[‡] Colgate-Palmolive R&D, Inc.
[§] Colgate-Palmolive Technology Center.

(1) Christov, N. C.; Denkov, N. D.; Kralchevsky, P. A.; Broze, G.; Mehreteab, A. *Langmuir* **2002**, *18*, 7880.
(2) Kralchevsky, P. A.; Denkov, N. D.; Todorov, P. D.; Marinov, G. S.; Broze, G.; Mehreteab, A. *Langmuir* **2002**, *18*, 7887.
(3) Chiu, Y. C.; Chang, C. Y. *J. Surf. Sci Technol.* **1990**, *6*, 349.
(4) Prak, D. J. L.; Abriola, L. M.; Weber, W. J., Jr.; Bocskay, K. A.; Pennell, K. D. *Environ. Sci. Technol.* **2000**, *34*, 476.
(5) McClements, D. J.; Dungan, S. R. *Colloids Surf., A* **1995**, *104*, 127.
(6) Coupland, J. N.; Brathwaite, D.; Fairley, P.; McClements, D. J. *J. Colloid Interface Sci.* **1997**, *190*, 71.

10.1021/la020367c CCC: $22.00
Published on Web 09/21/2002

to characterize the rate of solubilization with the time needed for the turbidity to level off.[3] More detailed kinetic information can be obtained if the time dependencies of the drop size and concentration are detected by dynamic and static light scattering.[5,6] Another method is to take samples from the shaken emulsion at selected times and to subject these samples to phase separation using a centrifuge: the kinetics of solubilization is characterized by the decrease of the volume of the separated oily phase for subsequent samples.[4] It should be noted that the interpretation of experimental results on solubilization kinetics with emulsions may face difficulties if there is flocculation, coalescence, or Ostwald ripening in the system.

Another approach to the solubilization kinetics, which avoids the aforementioned difficulties, is to carry out experiments with *single oil drops*. Carroll[7,8] developed a drop-on-fiber technique, which is based on the measuring the time dependence of the key dimensions of a drop attached to a fiber and having a constant nonzero contact angle. The method has been applied to the solubilization of various oils in different surfactant solutions. Ward[9] reviewed the individual and joint studies that he and Carroll undertook using this technique with ionic and nonionic surfactants. An alternative solubilization technique dealing with single oil drops has been developed and applied by Miller et al.[10−12] This is the basic-oil-drop contacting procedure, which uses a thin needle to inject small oil drops, typically 50−100 μm in diameter, into a rectangular glass capillary cell having a thickness of 400 μm and filled with the aqueous surfactant solution of interest. The diminishing of the oil drop was observed and recorded using videomicroscopy. An experimental technique, which is similar to that in refs 10−12, is used in our present study.

The paper is organized as follows. In section 2 we describe the used materials and solutions. In section 3 we present the two cells employed in our experiments, the "simple solubilization cell" and the "capillary cell", and compare their advantages and disadvantages. In section 4 we report experimental data about the effect of additives, such as ionic and zwitterionic surfactants and block copolymers, on the solubilization rate in nonionic surfactant solutions. Section 5 presents a systematic study on the effect of Synperonic L61 on the solubilization kinetics. The experimental data are processed by means of the theoretical model developed in ref 2, and the results are interpreted having in mind the micelle properties examined in ref 1.

2. Materials and Solutions

2.1. Surfactants. We carried out experiments with two nonionic surfactants: pentaoxyethylene monododecyl ether, $C_{12}E_5$ (Fluka), molecular mass M_w = 406.6; hexaoxyethylene monododecyl ether, $C_{12}E_6$ (Fluka), M_w = 450.6. In all solubilization experiments reported in this paper, we used 0.01 M NaCl solution for $C_{12}E_5$, and 0.2 M Na_2SO_4 solution for $C_{12}E_6$. In particular, 0.01 M NaCl was added to the $C_{12}E_5$ solutions for having a well-defined ionic strength, whereas 0.2 M Na_2SO_4 was added to the $C_{12}E_6$ solutions for enhancing the solubilization rate owing to the salting-out effect.

To examine the effect of micelle electric charge on the solubilization rate, in some experiments we added ionic and zwitterionic surfactants to the basic nonionic surfactant. In these experiments we used the anionic surfactant sodium dodecyl dioxyethylene sulfate (SDP2S), Empicol ESB70, Albright & Wilson Ltd. (Warley, U.K.), and the zwitterionic surfactant lauryldimethylamine oxide, $CH_3(CH_2)_{11}(CH_3)_2N^+O^-$, which will be referred to in the text as AO.

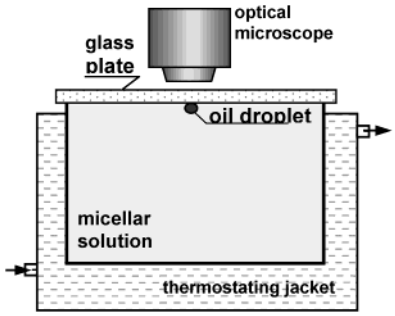

Figure 1. Sketch of cell no. 1, a setup for investigating the solubilization rate of individual oil drops, situated below a glass/water interface, by using optical microscopy.

2.2. Triblock Copolymers and Oils. Other additives, whose effect on the solubilization rate was examined, were $E_n-P_m-E_n$ triblock copolymers, where "E" stands for ethylene oxide (C_2H_4O), and "P" denotes propylene oxide (C_3H_7O). These are Synperonic PE/L61 (briefly SL61) with structure $E_{2.5}-P_{34}-E_{2.5}$, $M_w \approx 2100$, and Synperonic PE/L31 (briefly SL31) with structure $E_{1.2}-P_{18}-E_{1.2}$, $M_w \approx 1100$, both of them products of ICI. The mixed solutions of $C_{12}E_n$ (n = 5, 6) and triblock copolymer were prepared in the following way. First, the electrolyte was dissolved in water and the solution was filtered through 100 nm filter (Millex VV, Millipore). Then stock solutions, containing a mixture of $C_{12}E_n$ and copolymer of a desired molar ratio, were prepared by dissolving the necessary amounts of the two surfactants in the respective electrolyte solution. On the next day, the stock solution was diluted to the required surfactant concentration. Thus, a set of solutions of different total surfactant concentration were prepared at a constant electrolyte concentration and a fixed $C_{12}E_n$-to-copolymer ratio.

In most of our experiments, the solubilized oil was triolein (Nu-Chek. Prep. Inc.), M_w = 885. In comparative experiments we used also soybean oil, which was purified by passing through a column with the adsorbent Florisil. In this way, possible impurities from mono- and diglycerides, free fatty acids, and phospholipids were removed. The triolein contains C=C double bonds, which could be affected by oxidation and ester linkages that could be altered by keeping the lipid in aqueous medium. These processes are relatively slow (they take weeks and months) in comparison with our experiments on kinetics of solubilization of maximum duration 2−3 days.

All measurements were carried out at 27 °C. The glassware was cleaned by chromic acid and rinsed with deionized water from Milli-Q water purification system (Millipore Inc.).

3. Experimental Cells

3.1. Simple Solubilization Cell (Cell No. 1). In some of our solubilization experiments we used the experimental cell depicted in Figure 1. The micellar surfactant solution is placed in a thermostated glass vessel (of dimensions 2 × 2 × 1.5 cm), which is covered with a horizontal optical glass plate. The oil drops are prepared in the form of a diluted emulsion. Further, a small portion of this emulsion, 0.5−2 μL, is added by a pipet to the micellar solution, which is then covered by the glass plate. In this way only several oil drops are introduced in the cell. They emerge owing to the buoyancy force and stop below the glass plate (Figure 1). The drop radius is typically around and below 30 μm. Such drops are almost spherical in shape (negligible gravitational deformation). They do not stick to the glass plate: they are separated from the glass by an aqueous film. Due to the solubilization, the drop size diminishes

(7) Carroll, B. J. *J. Colloid Interface Sci.* **1976**, *57*, 488.
(8) Carroll, B. J. *J. Colloid Interface Sci.* **1981**, *79*, 126.
(9) Ward, A. J. I. In *Solubilization in Surfactant Aggregates*; Christian, S. D., Scamehorn, J. F., Eds.; M. Dekker: New York, 1995; Chapter 7.
(10) Lim, J.-C.; Miller, C. A. *Langmuir* **1991**, *7*, 2021.
(11) Chen, B.-H.; Miller, C. A.; Garrett, P. R. *Colloids Surf., A* **1997**, *128*, 129.
(12) Chen, B.-H.; Miller, C. A.; Garrett, P. R. *Langmuir* **1998**, *14*, 31.

with time. The drop diameter is monitored by using an optical microscope, Optiphot-2, Nikon (Tokyo, Japan), equipped with long-focus objectives, ×100 and ×32.

In general, the diminishing of the drops is very slow: it takes days for their complete solubilization. The experimental time dependence of the drop radius, $R(t)$, during the first several hours of solubilization can be fitted with a straight line:

$$R(t) = R_0 - At \tag{3.1}$$

Here R_0 is the initial drop radius. The slope, $A = -\mathrm{d}R/\mathrm{d}t$, of the experimental lines can be used as a characteristic of the solubilization rate. However, the experiments show that $\mathrm{d}R/\mathrm{d}t$ depends on R_0; consequently, one has to compare $\mathrm{d}R/\mathrm{d}t$ for drops with the same R_0 to reveal the relative solubilization rate of different micellar solutions. The latter fact makes $\mathrm{d}R/\mathrm{d}t$ a not very convenient characteristic of the solubilization kinetics.

The plot of the data as R^2 vs t gives also straight lines, whose slope again depends on R_0. If the solubilization occurs under a purely diffusion control, then one can derive (see Appendix B)

$$R^2(t) = {R_0}^2 - (2v_e c_{10} D_1)\, t \tag{3.2}$$

where it is assumed that the collision of an empty micelle with the oil−water interface leads to the solubilization of volume v_e from the oil drop; c_{10} and D_1 are respectively the bulk concentration and the diffusivity of the empty micelles. Note that, according to eq 3.2, the slope of the dependence R^2 vs t should be independent of the initial drop radius R_0, in contradiction with the experiment. One of the reasons for this deviation from diffusion-controlled kinetics is the presence of free thermal convection in cell no. 1, as discussed below.

A criterion about the presence or absence of thermally driven convections in the solution is provided by the Rayleigh number,[13]

$$R_a \equiv g\beta_e \Theta h^3/(\nu\chi) \tag{3.3}$$

where h is the height of the liquid in the vessel, g is the acceleration due to gravity, $\beta_e = 2.27 \times 10^{-4}\ \mathrm{K}^{-1}$ is the coefficient of thermal expansion of water, Θ is the characteristic temperature difference, $\nu \approx 8.2 \times 10^{-3}\ \mathrm{cm}^2/\mathrm{s}$ is the kinematic viscosity of water, and $\chi \approx 1.44 \times 10^{-3}\ \mathrm{cm}^2/\mathrm{s}$ is the thermal diffusivity of water. For $R_a \leq 1$ the free thermal convections are suppressed, whereas for $R_a > 1$ one could expect the presence of such convections. It is worthwhile noting that even with a fine control of the temperature, $\Theta \approx 0.2$ K, the Rayleigh number is rather large for the experimental cell from Figure 1, whose height is $h = 1.5$ cm: from eq 3.3 one calculates $R_a = 1.0 \times 10^4$. Hence, considerable free thermal convections take place in cell no. 1. In fact, it is virtually impossible to suppress the convections by thermostating of a centimeter-sized vessel. Instead, one could successfully suppress the free convections by decreasing the vertical dimension of the vessel, h (see ref 14 and the sources cited therein). Convection-free conditions can be accomplished in horizontal narrow capillaries, such as those used in the solubilization setup of Lim and Miller[10] and in that described in the next subsection.

(13) Landau, L. D.; Lifshitz, E. M. *Fluid Mechanics*; Pergamon Press: Oxford, U.K., 1984.

(14) Mysels, K. J. *Langmuir* **1992**, *8*, 3191.

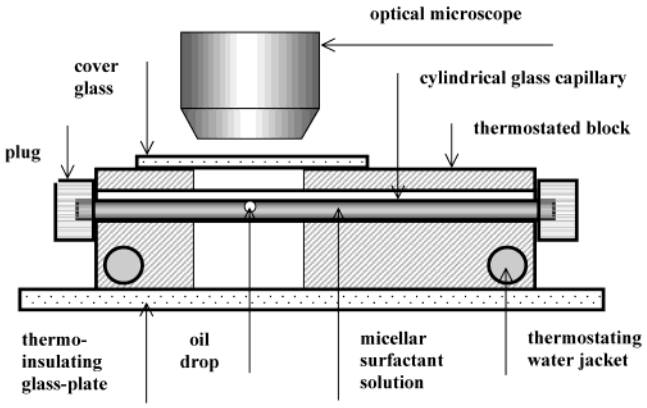

Figure 2. Sketch of the capillary cell (cell no. 2) for studying the kinetics of solubilization of individual oil drops. The diameter of the diminishing drop is recorded as a function of time.

3.2. Capillary Cell (Cell No. 2). The surfactant solution is loaded in a glass capillary of inner diameter 585 μm and length 50 mm. The loading is accomplished by immersion of one of the capillary ends in the solution, which spontaneously fills the tube due to the capillary-rise effect. Next, the capillary is inserted in a horizontal cylindrical channel drilled in the thermostated metal block of the experimental setup (Figure 2). An oil drop is injected in the capillary by means of a microsyringe with a fine glass needle of outer diameter 45 μm. The drop radius is typically $R \leq 50$ μm. After that, the two ends of the capillary are plugged to prevent evaporation of the solution. During the experiment, the capillary is held in the horizontal channel; the temperature is maintained at 27 °C. The metal block has 8 parallel channels, which allow simultaneous experiments with 8 capillaries. Above each capillary, there is an opening, covered with a glass plate, which enables one to observe the oil drops by an optical microscope (Figure 2). Thus, the diminishing of each oil drop, due to solubilization, can be recorded as a function of time. To clean the capillaries, we filled them for at least 12 h with a solution of sulfochromic acid, followed by a subsequent abundant rinsing by deionized water.

The relatively small inner diameter of the capillary, and its horizontal position, prevent the appearance of free thermal convections in the surfactant solution; the Rayleigh number, calculated from eq 3.3, is $R_a = 0.6$. Hence, one may expect that the free thermal convections are suppressed and the solubilization happens under barrier-diffusion control. If some uncontrollable thermal convections were present, they would make impossible to quantitatively interpret the experimental data.

The absence of thermal convections in the capillary cell (Figure 2) was proven in experiments with benzene drops, reported elsewhere.[15] In brief, a benzene drop is injected in the capillary, which is filled with a surfactant solution at concentration below the cmc (no micellar solubilization). Such a drop diminishes due to molecular dissolution of the benzene in water. If convections are missing, the process is described by the equation

$$R(t) = [1.8\beta_1(t_0 - t)]^{1/2} \tag{3.4}$$

where t_0 is the moment of drop disappearance, $R(t_0) = 0$, and β_1 is a known material parameter; for benzene $\beta_1 = 1.65 \times 10^{-8}\ \mathrm{cm}^2/\mathrm{s}$. Our experiments showed that eq 3.4

(15) Todorov, P. D.; Kralchevsky, P. A.; Denkov, N. D.; Broze, G.; Mehreteab, A. *J. Colloid Interface Sci.* **2002**, *245*, 371.

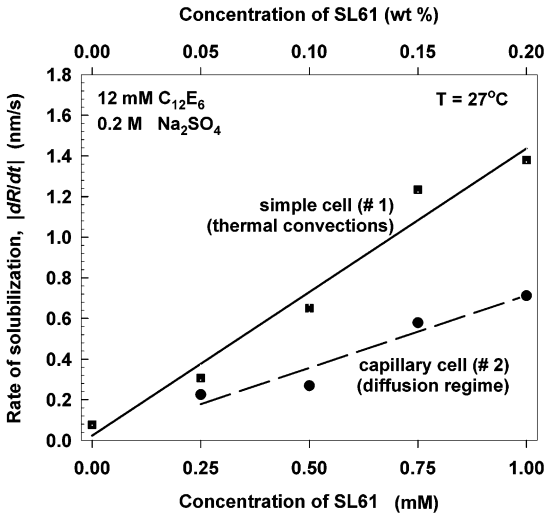

Figure 3. Rate of solubilization of soybean oil vs the concentration of triblock copolymer SL61. The upper and lower curves represent experimental results obtained by means of cells nos. 1 and 2, respectively. All solutions contain 12 mM EO6 + 0.2 M Na_2SO_4 at temperature 27 °C.

excellently agrees with the experimental data (no adjustable parameters), which proves the absence of free thermal convections in the capillary-cell setup.[15]

In conclusion, the capillary cell (cell no. 2) enables one to obtain experimental data on kinetics of solubilization, which can be further interpreted by means of the theory developed in ref 2. The simple cell (cell no. 1) is easier to operate and gives data about the relative rate of solubilization in various solutions. On the other hand, the results obtained by cell no. 1 are affected by uncontrollable thermal convections and are not liable to a quantitative theoretical interpretation.

As an illustration, in Figure 3 we present data for the solubilization rate of soybean-oil drops characterized by $|dR/dt|$. All drops have initial radius $R_0 \approx 35 \pm 5\ \mu$m; the scattering of the points is due to the scattering in the values of R_0. The data demonstrate that the solubilization rate increases with the concentration of the added triblock copolymer SL61. The rates measured with cell no. 1 are systematically larger than those obtained with cell no. 2, as it could be expected. The difference can be attributed to the presence of thermal convections in cell no. 1.

4. Effect of Additives on the Solubilization Rate

4.1. Addition of Ionic Surfactant. As mentioned in the Introduction, if the solubilization of triglycerides by nonionic surfactant solutions occurs through transient attachments of micelles to the oil−water interface, then every factor which impedes the micelle adsorption would lead to suppression of the process or to its complete ceasing. As discussed by Chen et al.,[11] such a factor is the electrostatic repulsion between the micelles and the oil−water interface, the latter being covered with a surfactant adsorption monolayer, which bears an electric charge similar to that of the micelles.

To examine the effect of electrostatic repulsion with our system, we added various portions of the anionic surfactant SDP2S to the solution of 12 mM $C_{12}E_6$ + 0.2 M Na_2SO_4. Thus, the molar fraction of SDP2S in the surfactant blend,

$$X_{SDP2S} = C_{SDP2S}/(C_{C12E6} + C_{SDP2S}) \qquad (4.1)$$

was varied (C denotes molar concentration). The addition

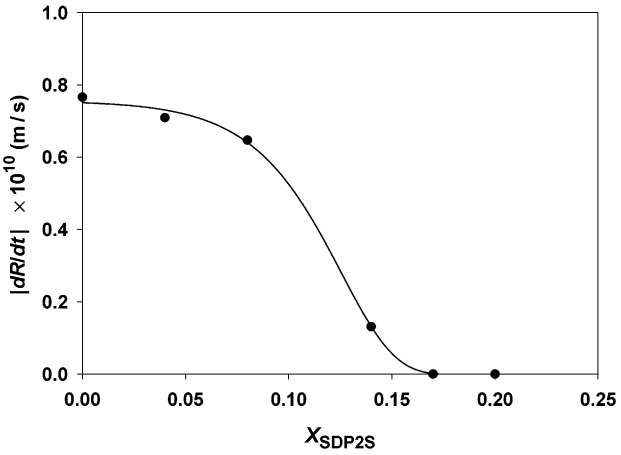

Figure 4. Rate of solubilization of soybean oil vs the mole fraction of SDP2S in mixture with $C_{12}E_6$. All solutions contain 12 mM $C_{12}E_6$ and 0.2 M Na_2SO_4. The experiments are carried out with separate oil drops of initial radius $R_0 \approx 35\ \mu$m in cell no. 1 (Figure 1).

of SDP2S to the $C_{12}E_6$ solutions does not significantly affect the micelle size: by means of dynamic light scattering (DLS; Malvern 4700C, Malvern, U.K.) we found that the hydrodynamic diameter of the empty micelles varies within 10% for $0 \le X_{SDP2S} \le 0.25$.

Figure 4 shows the rate of solubilization of soybean oil, characterized by $|dR/dt|$, as a function of X_{SDP2S}. The results demonstrate that the solubilization rate considerably decreases for $X_{SDP2S} \ge 0.10$; furthermore, the solubilization is completely ceased for $X_{SDP2S} \ge 0.17$. These findings can be attributed to a growth of the electrostatic barrier to micelle adsorption and to a decrease in the respective adsorption energy, caused by the rise of the negative surface electric charge. Our results are consonant with the findings of other authors[11,16−19] that the solubilization is suppressed in the presence of ionic surfactants, except in the case of oils which exhibit a considerable solubility in pure water.[15]

On the other hand, ionic surfactants are most frequently involved in detergency formulations because of their useful properties.[20] One way to diminish their inhibitory action on solubilization is considered in the next subsection.

4.2. Addition of Zwitterionic Surfactant. Zwitterionic surfactants, such as the amine oxides, are known to increase the skin compatibility of detergent products. They have also foam boosting and/or stabilizing properties. With anionics, the amine oxides form complexes, which show greater surface activity than either of the constitutive surfactants.[20] Moreover, these complexes are electroneutral—the latter property can be employed to neutralize the inhibitory action of anionic surfactants (such as SDP2S) on solubilization. With this end in view, we added various portions of lauryldimethylamine oxide (AO) to the blend of $C_{12}E_6$ + SDP2S. The basic solution contained 12 mM $C_{12}E_6$ + 0.2 M Na_2SO_4 + 2 or 3 mM SDP2S.

First, we checked how the addition of AO affects the surface electric potential. To do that we measured the ζ-potential of soybean oil drops, covered with surfactant adsorption monolayer, as a function of the mole fraction

(16) Bolsman, T. A. B. M.; Veltmatt, F. T. G.; van Os, N. M. *J. Am. Oil Chem. Soc.* **1988**, *65*, 280.
(17) Kabalnov, A. S. *Langmuir* **1994**, *10*, 680.
(18) Taylor, P. *Colloids Surf., A* **1995**, *99*, 175.
(19) Soma, J.; Papadopulos, K. D. *J. Colloid Interface Sci.* **1996**, *181*, 225.
(20) Oldenhove de Guertechin, L. In *Handbook of Detergents, Part A: Properties*; Broze, G., Ed.; M. Dekker: New York, 1999; Chapter 2.

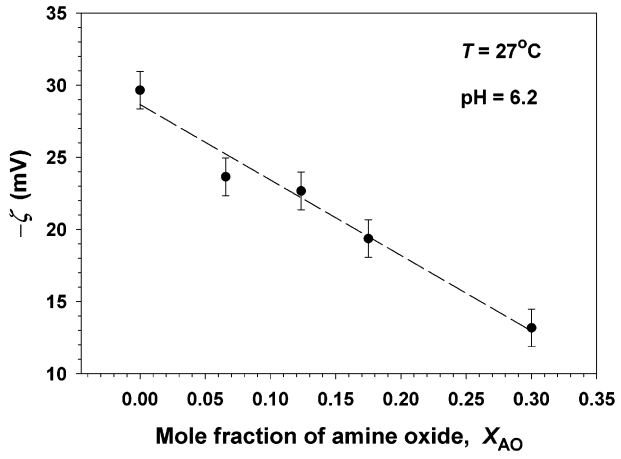

Figure 5. ζ-potential of soybean oil drops vs the mole fraction of amine oxide, X_{AO}, in mixture with $C_{12}E_6$ and SDP2S. All solutions contain 0.4 mM $C_{12}E_6$ + 0.067 mM SDP2S + 6.67 mM Na_2SO_4. The line is a guide to the eye.

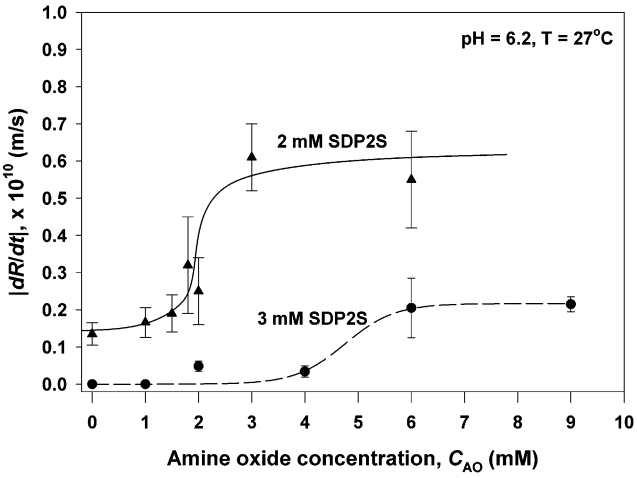

Figure 6. Solubilization rate of soybean oil drops vs the concentration of amine oxide, C_{AO}, in mixed surfactant solution containing 12 mM $C_{12}EO_6$, 0.2 M Na_2SO_4, and SDP2S. (The triangles and circles correspond to 2 and 3 mM SDP2S, respectively.) The experiments are carried out in cell no. 1 at T = 27 °C for initial drop radius $R_0 \approx 35$ μm. The lines are guides to the eye.

of AO in the surfactant blend,

$$X_{AO} = C_{AO}/(C_{C12E6} + C_{SDP2S} + C_{AO}) \qquad (4.2)$$

The measurements of ζ-potential were carried out by means of a Zetasizer II C (Malvern Instruments, U.K.). Due to technical reasons, the ionic strength of the solution must be less than 50 mM. Therefore, in our ζ-potential experiments, the basic solution with 2 mM SDP2S was diluted 30 times; that is, we worked with a solution containing 0.4 mM $C_{12}E_6$ + 0.067 mM SDP2S + 6.67 mM Na_2SO_4. The results, presented in Figure 5, show a significant decrease of the negative surface potential with the rise of X_{AO}. This is an indication about the formation of the electroneutral complex AO−SDP2S. The resulting suppression of the electrostatic (double layer) repulsion is expected to promote the solubilization.

Figure 6 shows the rate of solubilization of soybean oil, characterized by $|dR/dt|$, as a function of the concentration of added amine oxide, C_{AO}. The results demonstrate that the solubilization rate increases after C_{AO} reaches a certain threshold value and then levels off with the further increase of C_{AO}. The accelerating effect of AO on solubilization is greater for the solution with lower concentration of the ionic surfactant, that with 2 mM SDP2S. The highest value of the solubilization rate in Figure 6, $|dR/dt| \approx 0.06$ nm/s, is still lower than the respective value in the absence of AO and SDP2S, viz. $|dR/dt| \approx 0.08$ nm/s for the solution containing 12 mM $C_{12}E_6$ + 0.2 M Na_2SO_4. Hence, we may conclude that the addition of AO partially compensates the inhibitory effect of SDP2S on solubilization. However, at least in our case, the solutions containing nonionics alone exhibit a better solubilization performance than the mixtures of nonionic + anionic + amine oxide.

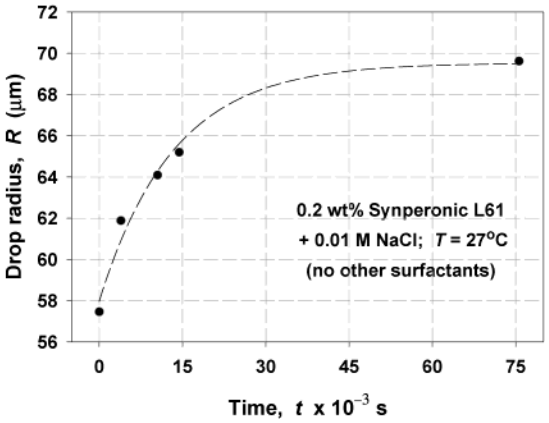

Figure 7. Plot of the drop radius R vs time t. Experimental data were obtained in cell no. 2 for a triolein drop in 0.2 wt % aqueous solution of SL61 + 0.01 M NaCl and no other surfactants.

4.3. Addition of Triblock Copolymers. As demonstrated in Figure 3, the addition of the triblock copolymer SL61 essentially accelerates the solubilization of soybean oil by solutions of the nonionic surfactant $C_{12}E_6$. In ref 1 it has been established that in the mixed solutions of $C_{12}E_6$ and SL61 large cylindrical micelles are formed, each of them containing hundreds to thousands surfactant molecules and dozens of copolymer molecules. The rest of this paper is devoted to investigation of the accelerating effect of triblock copolymers on the solubilization of triglycerides.

It is known that some of the $E_n-P_m-E_n$ copolymers form micelles in water, in the absence of any other surfactant. To check whether aqueous solutions of SL61 alone are able to solubilize triglycerides, we carried out experiments with separate oil drops by means of the capillary cell (Figure 2). Instead of diminishing, we observed a growth in the size of the oil drop. An example is shown in Figure 7 for a triolein drop in an aqueous solution of 0.2 wt % SL61 + 0.01 M NaCl. One sees that the drop radius increases with about 20% for 10 h and reaches an equilibrium value. This behavior can be attributed to a transfer of SL61 molecules from the aqueous into the oil phase, with a subsequent equilibration.

In the presence of nonionic surfactants, such as $C_{12}E_5$ and $C_{12}E_6$, the triblock copolymers SL31 and SL61 are retained in the aqueous phase in the form of mixed micelles with the nonionic.[1] Figure 8 shows the rate of solubilization of triolein, characterized by the rate of diminishing of the drop radius, $|dR/dt|$, as a function of the concentration of added copolymer. The results demonstrate that SL61 is a much better promoter of solubilization than SL31. Indeed, it turns out that the solubilization rate of triolein, $|dR/dt|$, is about 3 times greater in the solutions containing SL61, in comparison with the solutions of SL31, at the same weight concentration. The reason for this difference is not yet clarified, but it is most probably connected with

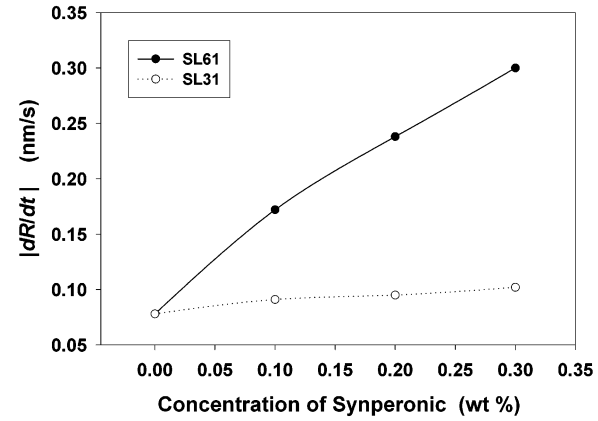

Figure 8. Comparison of the solubilization rates in the presence of SL61 and SL31 in solutions containing 12 mM $C_{12}E_5$ + 0.01 M NaCl. The experiments are carried out with separate triolein drops of initial radius $R_0 \approx 48$ μm in cell no. 2.

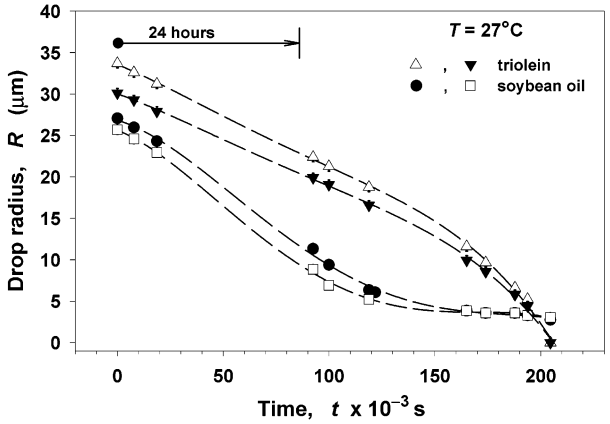

Figure 9. Solubilization of drops from triolein (triangles) and soybean oil (circles and squares) in surfactant solution containing 12 mM $C_{12}E_6$ + 0.25 mM (0.05 wt %) SL61 + 0.2 M Na_2SO_4 shown as a plot of drop radius vs time. The experiments are performed in cell no. 2.

the structure and properties of the formed mixed micelles which, in turns, depend on the compatibility of the hydrophilic and hydrophobic moieties of the surfactant and copolymer molecules.

The type of triglyceride can also affect the solubilization rate. Figure 9 shows comparative experiments with triolein and soybean oil drops in aqueous solution of 12 mM $C_{12}E_6$ + 0.05 wt % SL61 + 0.2 M Na_2SO_4. One sees that, during the first day, the drop radius, R, decreases almost linearly with time. However, at longer times the dependence $R(t)$ exhibits a nonlinear behavior: the diminishing of the drops is accelerating for the triolein but decelerating for the soybean oil (Figure 9). In the next section 5 it is shown that the experimental dependence $R(t)$ for the triolein drops agrees very well with the theoretical predictions and with the results from independent NMR measurements. For that reason, the different shape of the $R(t)$ dependence in the case of soybean oil is explained by the complex composition of this oil, which is a mixture of components having various molecular weight. Indeed, one can expect that the lighter fractions of the soybean oil are first solubilized; simultaneously, the heavier fractions are progressively concentrated in the diminishing oil drop, which decelerates the solubilization.

To avoid problems with the complex composition of the soybean oil, in our detailed study (section 5) we work only with triolein drops. As an additive we chose SL61, which turns out to be the best promoter of solubilization among the substances investigated by us.

5. Detailed Study of the Effect of SL61

5.1. Theoretical and Experimental *R(t)* Dependence. As already mentioned, the rate of diminishing of the drop radius, $|dR/dt|$, is not the most convenient characteristics of the solubilization rate, insofar as $|dR/dt|$ depends on the initial drop radius, R_0. In such a case, to investigate the solubilization properties of solutions at various concentrations and compositions, one has to form many oil drops with the same R_0, which is not so easy. From the viewpoint of comparison between theory and experiment, the best way is to fit the experimental time dependence of drop radius, $R(t)$, with the theoretical expression

$$R(t) = \frac{\alpha}{\beta}\{[1 + 2\beta(t_0 - t)]^{1/2} - 1\} \quad t \le t_0 \qquad (5.1)$$

The detailed derivation of eq 5.1 is the subject of part 2 of this series.[2] Equation 5.1 describes the solubilization of an oil drop in the general case of mixed barrier-diffusion control (the capillary cell, sketched in Figure 2, provides the respective conditions). α and β are parameters, which are independent of R and t, but are related to the properties of the micellar solution; see eq 5.3. The moment $t = t_0$ corresponds to $R = 0$, that is, to the drop disappearance. From eq 5.1 we obtain

$$\left|\frac{dR}{dt}\right|_{t=0} = \frac{\alpha}{1 + (\beta/\alpha)R_0} \qquad (5.2)$$

where $R_0 = R(t = 0)$ is the initial drop radius. Equation 5.2 explains why the initial rate of drop diminishing is greater for smaller R_0. The best way to determine the parameters α and β is to process simultaneously the data for several diminishing oil drops (at the same composition of the micellar solution) by means of eq 5.1. The respective numerical procedure for data processing is described in Appendix A. Figure 10 shows some illustrative experimental data and their fits by means of eq 5.1.

Having determined the parameters α and β from the fits, one can calculate the average number of oil molecules solubilized in a swollen micelle, n_s, and the compound rate constant of solubilization, χ:

$$n_s = \frac{1}{\lambda m c_{10} D_1 v_o}\frac{\alpha^2}{\beta} \qquad \chi = \frac{\beta}{\alpha}D_1 \qquad (5.3)$$

See ref 2 for details. Here, $\lambda = 0.9$ is a geometric correction factor, m is the average number of swollen micelles obtained by splitting of a larger empty micelle in the course of solubilization,[21] D_1 is the diffusivity of the empty micelles, v_o is the volume occupied by an oil molecule in the oily phase, and c_{10} is the bulk number concentration of empty micelles in the solution.

5.2. Experimental Results. From the mass density and molecular weight of triolein, we calculate $v_o = 1.63$ nm^3. The values of D_1 and c_{10} depend on the solution's concentration and composition. In Table 1 we list values of D_1 and c_{10}, which are obtained by light scattering experiments (see ref 1 for details). In particular, the values of D_1 are directly obtained by dynamic light scattering. To determine c_{10} we first determined by static light scattering the number of surfactant molecules per micelle, $N_{surfact.}$;

(21) Hoffmann, H.; Ulbricht, W. *J. Colloid Interface Sci.* **1989**, *129*, 388.

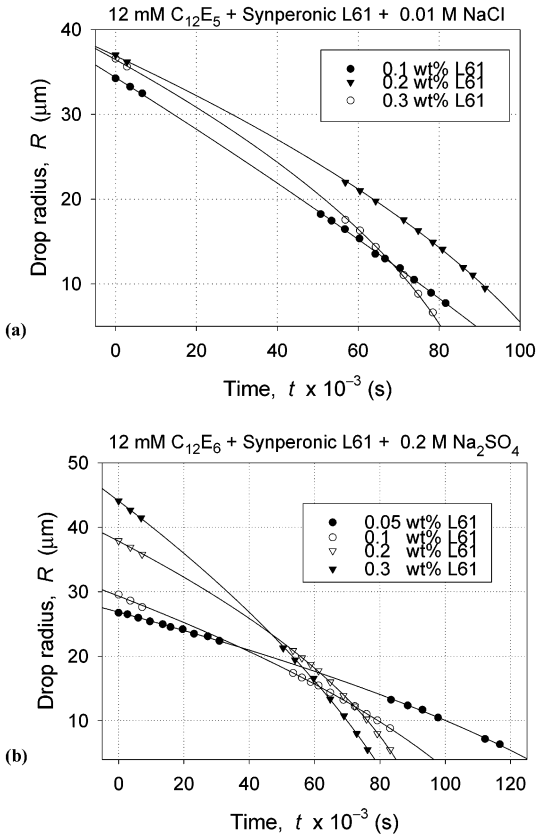

Figure 10. Plots of the radius, R, of triolein drops vs time, t, with results from solubilization experiments in cell no. 2 at temperature 27 °C and various concentrations of SL61 denoted in the figure. The micellar solutions are (a) 12 mM $C_{12}E_5$ + 0.01 M NaCl + SL61 and (b) 12 mM $C_{12}E_6$ + 0.2 M Na_2SO_4 + SL61. The lines are best fits by means of eq 5.1.

Table 1. Experimental Parameters for the Empty Micelles

Synperonic L61 C_{SL61} (wt %)	diffusivity D_1 (cm^2/s)	micelle diameter d_h (nm) (eq 5.4)	micelle concn c_{10} (cm^{-3})
(a) Solutions of 0.012 M $C_{12}E_5$ + 0.01 M NaCl			
0.0	0.912×10^{-7}	47.7	
0.1	1.49×10^{-7}	34.7	3.91×10^{15}
0.2	1.93×10^{-7}	26.8	8.04×10^{15}
0.3	2.15×10^{-7}	24	9.95×10^{15}
(b) Solutions of 0.012 M $C_{12}E_6$ + 0.2 M Na_2SO_4			
0	2.20×10^{-7}	23.5	0.71×10^{16}
0.04	2.61×10^{-7}	19.8	0.98×10^{16}
0.05	2.71×10^{-7}	19.1	1.05×10^{16}
0.08	2.99×10^{-7}	17.3	1.27×10^{16}
0.10	3.08×10^{-7}	16.8	1.39×10^{16}
0.15	3.3×10^{-7}	15.5	1.70×10^{16}
0.20	3.45×10^{-7}	14.7	2.02×10^{16}

then we calculate $c_{10} = (c_s - \text{cmc})/N_{\text{surfact.}}$, where c_s is the total surfactant concentration. (Values of $N_{\text{surfact.}}$ for empty micelles are given in ref 1, Table 1.)

To illustrate the values in Table 1, in Figure 11 we present the effective hydrodynamic diameter, d_h, which is defined by means of the Stokes−Einstein formula

$$d_h = kT/(3\pi\eta D_1) \qquad (5.4)$$

(k = Boltzmann constant; η = viscosity of water). In fact, d_h is the diameter of an imaginary spherical particle, which has the same diffusivity D_1 as the real elongated micelle. Figure 11 shows that the micelle size considerably decreases with the rise of the SL61 concentration. Moreover, the empty micelles in the investigated solutions

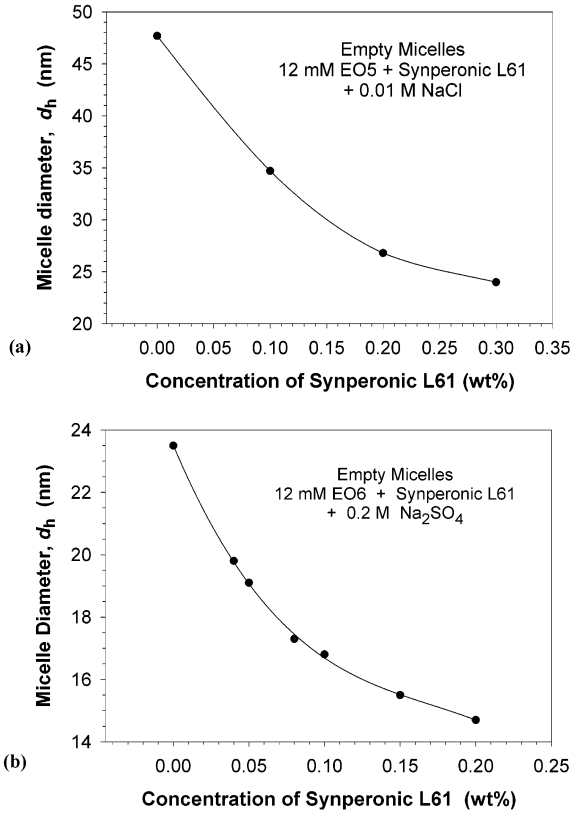

Figure 11. Hydrodynamic diameter d_h of the empty micelles vs the concentration of SL61 for solutions containing (a) $C_{12}E_5$ and (b) $C_{12}E_6$. The continuous lines are fits by parabola.

Table 2. Equilibrium and Kinetic Parameters Related to the Solubilization of Triolein Drops

C_{SL61} (wt %)	m	α (nm/s)	$10^6\beta$ (s^{-1})	χ (μm/s) (eq 5.3)	n_s (eq 5.3)	n_s (NMR)
(a) Solutions of 0.012 M $C_{12}E_5$ + 0.01 M NaCl						
0.0		0.14 ± 0.01	3 ± 1	0.20		
0.1	5.4	0.21 ± 0.01	4.7 ± 1	0.34	20	20 ± 3
0.2	3.5	0.68 ± 0.03	37 ± 5	1.05	16	15 ± 2
0.3	3.1	1.05 ± 0.07	85 ± 14	1.74	13	12 ± 2
(b) Solutions of 0.012 M $C_{12}E_6$ + 0.2 M Na_2SO_4						
0.0	3.0	0.034 ± 0.01	0.34 ± 0.06	0.22	5	12 ± 2
0.05	2.7	0.33 ± 0.02	17 ± 3	1.40	6	10 ± 2
0.1	2.4	0.47 ± 0.03	22 ± 4	1.44	7	8 ± 1
0.2	1.8	0.53 ± 0.03	22 ± 4	1.43	7	9 ± 1

of $C_{12}E_5$ are markedly larger than those in the solutions of $C_{12}E_6$. Below these results will be discussed in relation to the solubilization kinetics in the respective solutions.

Note that, in the absence of SL61, the nonionic surfactant $C_{12}E_5$ forms giant branched threadlike micelles.[22] In all other cases we deal with elongated rodlike micelles. Since our procedure for processing the light-scattering data (see ref 1) is inapplicable to branched micelles, we could not determine c_{10} and m for the micelles of $C_{12}E_5$ in the absence of SL61.

Table 2 summarizes our results for the solubilization of triolein drops in micellar solutions of $C_{12}E_5$ and $C_{12}E_6$ with added various concentrations of SL61. The first column shows the concentration of SL61. The values of m (the number of swollen micelles obtained by splitting of an empty micelle upon solubilization) are obtained by analysis of the static light-scattering data in ref 1. The solubilization kinetic parameters α and β are determined

(22) Bernheim-Groswasser, A.; Wachtel, E.; Talmon, Y. *Langmuir* **2000**, *16*, 4131.

as adjustable parameters from the best fit of data for diminishing oil drops (cell no. 2) by means of eq 5.1; see Appendix A for details. Next, the compound solubilization rate constant, χ, and the number of triolein molecules/swollen micelle, n_s, are calculated from the respective values of α and β by using eq 5.3. For comparison, the last column of Table 2 contains values of n_s, which have been obtained in an independent way, by means of NMR spectroscopy in combination with static light scattering; for details see ref 1. Note that the parameters m and n_s (NMR) are obtained in *equilibrium* experiments (triolein phase equilibrated with the micellar solution), whereas the parameters α and β are determined in *kinetic* experiments with separate diminishing triolein drops in cell no. 2.

5.3. Discussion. As mentioned above, the initial rate of diminishing of the drop radius, $|dR/dt|_{t=0}$, is not the most appropriate characteristics of the solubilization rate because it depends on the initial drop radius, R_0; see eq 5.2. In our opinion, an adequate characteristics of the solubilization rate is given by the kinetic parameter α, which is independent of the drop size. In fact, $\alpha = |dR/dt|$ for sufficiently small drops; that is, in the limiting case $(\beta/\alpha)R \ll 1$ (see eq 5.2). If α is accepted as a measure of the solubilization rate, from Table 2 we can conclude that the addition of SL61 to the solutions of nonionic surfactants strongly accelerates the solubilization. For example, the addition of 0.2 wt % SL61 increases the solubilization rate of triolein in the investigated solutions of $C_{12}E_5$ and $C_{12}E_6$ respectively 5 and 15 times.

The compound solubilization kinetic constant χ also exhibits a tendency to increase with the rise of the SL61 concentration (Table 2). This parameter can be expressed in the form[2]

$$\chi = \frac{k_{1,a}}{1 + k_{1,d}/k_s} \tag{5.5}$$

where $k_{1,a}$ and $k_{1,d}$ are the rate constants of adsorption and desorption of empty micelles at the oil−water interface and k_s is the rate constant of the uptake of oil, that is, of the reaction

$$\{\text{empty micelle}\} + \{\text{oil molecules}\} = m\{\text{swollen micelles}\} \tag{5.6}$$

which takes place at the interface. If the latter reaction is sufficiently fast, i.e., if $k_s \gg k_{1,d}$, eq 5.5 predicts $\chi \approx k_{1,a}$, which means that the total solubilization rate is limited by the rate of adsorption of the empty micelles. If this is the case, all adsorbed empty micelles will be completely transformed into "equilibrated" swollen micelles, before their desorption (insofar as $k_s \gg k_{1,d}$). The coincidence of the data for n_s in the last two columns of Table 2a indicates that this is really the case for the investigated solutions of $C_{12}E_5$. Indeed, eq 5.3 gives a kinetic value of n_s, determined from the time dependence, $R(t)$, of the radius of diminishing oil drops; see Figure 10. On the other hand, the value of n_s obtained by means of NMR refers to micellar solutions which have been equilibrated with the oil phase. Moreover, the good agreement between the data for n_s in the last two columns of Table 2a is an argument in favor of the correctness of our theoretical interpretation of the light-scattering data about the mixed micelles, as well as of the data for diminishing oil drops obtained in cell no. 2.

As discussed above, for the solutions of $C_{12}E_5$, we have $\chi \approx k_{1,a}$. The rate constant of micelle adsorption can be expressed in the form $k_{1,a} = P \exp(-E_a/kT)$, where P is a preexponential factor and E_a is the activation energy; that is, the empty micelles encounter a barrier to adsorption of height E_a. In the considered case, it turns out that the magnitude of E_a controls the solubilization rate. Our model considerations in ref 2 showed that the height of the adsorption barrier is proportional to the length L of the rodlike micelles; that is, $E_a = wL$, where w is the activation energy/unit length of the rodlike micelle. Therefore, one may expect that

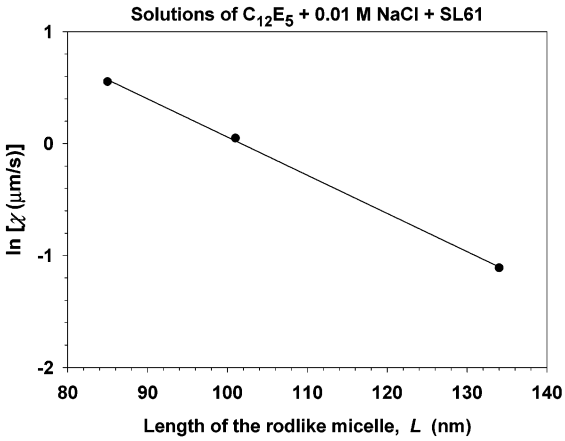

Figure 12. Plot of data from Table 2a for the compound solubilization rate constant, χ, vs the length, L, of the rodlike micelles, in accordance with eq 5.7.

$$\ln(\chi) \approx \ln(k_{1,a}) \approx A_1 - \frac{w}{kT}L \tag{5.7}$$

where A_1 and w are (in first approximation) constant parameters. To check whether our data complies with eq 5.8, in Figure 12 we have plotted $\ln(\chi)$ vs L; the values of χ are from Table 2a for $C_{SL61} = 0.1$, 0.2, and 0.3 wt %. The length of the empty micelles, $L = 2pa$, was computed using the values of p and a from Table 1 in ref 1 for $C_{12}E_5$. ($2a$ is the diameter of the cylindrical micelle, and p is the ratio of its length and diameter.) Figure 12 shows that our data really agree with eq 5.7. The slope yields $w = 0.034kT$/nm. Thus for micelles of length $L = 50$, 100, and 150 nm, the estimated height of the adsorption barrier is $E_a = 1.7kT$, $3.4kT$, and $5.1kT$, respectively.

The agreement of our data with eq 5.7 (Figure 12) implies that the addition of SL61 to the solution of nonionic surfactant decreases the length of the rodlike micelles, thus reducing the kinetic barrier to adsorption and accelerating the solubilization process. However, this is not the only way SL61 affects the solubilization rate. As mentioned earlier, the latter is characterized by the kinetic parameter α, which is defined as follows:[2]

$$\alpha = \lambda v_0 m n_s \chi c_{10} \tag{5.8}$$

The addition of SL61, at fixed concentration of $C_{12}E_n$, simultaneously increases χ and c_{10} but decreases m and n_s (see Table 2). In a final reckoning, the growth of the product χc_{10} prevails and determines the overall increase of α with the rise of the SL61 concentration.

In the case of $C_{12}E_6$, the solubilization rate α also increases with the rise of the SL61 concentration; see Table 2b. In this case the kinetic values of n_s are systematically lower than the equilibrium values of n_s determined by NMR (cf. the last two columns of Table 2b), the difference being larger for the lower concentrations of SL61. This result can be interpreted as follows.

Kinetic values of n_s, lower than the equilibrium ones, imply that the micelles may prematurely desorb from the oil−water interface, before the completion of the reaction 5.6, that is before taking the maximum possible amount of oil molecules/micelle. In view of eq 5.5, this means that the rate constants of desorption and solubilization are comparable; that is, the ratio $k_{1,d}/k_s$ is not much smaller than 1. Such a behavior could be attributed to the fact that the hydrophilic polyoxyethylene brushes of the adsorption layers (and micelles) from $C_{12}E_6$ are thicker and more hydrated than those from $C_{12}E_5$. Thus, the transport of a hydrophobic triolein molecule from the oil phase, across the hydrophilic brush and into an adsorbed micelle, encounters a higher kinetic barrier (smaller k_s) in the case of $C_{12}E_6$. In addition, a more hydrophilic brush implies a weaker adhesion of the micelles to the oil−water interface, that is, a greater desorption rate constant $k_{1,d}$. Both effects tend to increase the ratio $k_{1,d}/k_s$ for $C_{12}E_6$, in comparison with $C_{12}E_5$. The addition of SL61 seems to make the micelles and the adsorption layers more hydrophobic (that is more "sticky"), which has the opposite effect on the ratio $k_{1,d}/k_s$. This is indicated by the closer kinetic and equilibrium values of n_s for the higher concentrations of SL61 in Table 2b. The markedly strong increase of the solubilization rate with the rise of C_{SL61} (more than 15 times) in the case of $C_{12}E_6$ seems to be a manifestation of this "hydrophobizing action" of SL61.

6. Summary and Conclusions

In this paper we investigate the kinetics of solubilization of triglycerides (triolein and soybean oil) by observing the diminishing of individual oil drops (of radius $\leq 50\ \mu$m) in a micellar surfactant solution. Two solubilization cells were used: Cell no. 1 is a thermostated centimeter-sized glass vessel containing the investigated micellar solution and a few oil drops (Figure 1). Cell no. 2 represents a set of horizontal glass capillaries (inner diameter 585 μm) filled with the micellar solution (Figure 2). In each capillary, an oil drop is injected with the help of a syringe. Cell no. 1 is more easy to operate; it can be used to compare the solubilization rates for different systems at the same temperature and size of the oil drops. However, the solubilization rates measured in cell no. 1 are not liable to theoretical interpretation, because they are affected by the presence of slow, but uncontrollable, thermal convections in the solution (see Figure 3). The latter drawback is overcome in cell no. 2 owing to the small vertical dimension of the working space.

The two solubilization cells have been applied to examine the solubilization of triglycerides by micellar solutions of the nonionic surfactants $C_{12}E_5$ and $C_{12}E_6$. We investigated the effect of various additives on the solubilization rate. The addition of an anionic surfactant (SDP2S) was found to decelerate and completely suppress the solubilization (Figure 4). The latter effect can be attributed to the electrostatic repulsion between the micelles and the oil−water interface, which are charged due to the anionic surfactant. Its inhibitory action on solubilization can be partially removed by addition of an amphoteric surfactant, which makes an electroneutral complex with the anionic (Figure 6).

Highest solubilization rates have been achieved by addition of $E_n-P_m-E_n$ triblock copolymers (Synperonics) to the micellar solutions of the nonionics $C_{12}E_5$ and $C_{12}E_6$. In the absence of nonionic surfactant, the aqueous solution of copolymer does not solubilize oil, but instead, the copolymer is transferred into the oil phase (Figure 7). In contrast, the mixed solutions of nonionics and copolymer contain large rodlike micelles, which provide a relatively high solubilization rate. The latter is found to increase with the rise of the copolymer concentration (Figure 10). The obtained experimental data in cell no. 2 are found to agree very well with the theoretical time dependence of the drop radius, $R(t)$; see eq 5.1, Table 2, and Appendix A. From the best fits of the data we determined the solubilization rate, α, the compound kinetic constant of solubilization, χ, and the number of oil molecules/swollen micelle, n_s; see section 5. In particular, each swollen micelle detaches from the triolein−water interface after taking 5−20 triolein molecules, depending on the solution's composition.

The kinetic values of n_s, determined with diminishing oil drops, have been compared with the equilibrium values of n_s, independently obtained by NMR spectroscopy (Table 2). For the solutions containing $C_{12}E_5$, the kinetic and equilibrium n_s coincide, which implies that the adsorption of empty micelles at the oil−water interface is the time-limiting step of the solubilization. The addition of copolymer decreases the size of the mixed micelles (Figure 11), which, in this way, reduces the barrier to micelle adsorption (eq 5.7 and Figure 12) and accelerates the solubilization.

In the case of mixed solutions of $C_{12}E_6$, the kinetic values of n_s are smaller than the equilibrium ones (Table 2b). This can be attributed to the more hydrophilic poly(oxyethylene) brushes of the adsorbed $C_{12}E_6$ (in comparison with $C_{12}E_5$), which cause a premature desorption of the micelles from the oil−water interface, before taking the maximum portion of oil molecules. The addition of copolymer seems to make the micelles and the adsorption layers of $C_{12}E_6$ more hydrophobic (more sticky), which leads to a considerable increase of the solubilization rate (more than 15 times).

The results of this study could be helpful for the analysis and control of the solubilization kinetics of triglycerides and other water-insoluble oils.

Acknowledgment. The support by Colgate-Palmolive is gratefully acknowledged. The authors are indebted to Professor Krassimir Danov for his consultation concerning the data processing, as well as to Mrs. Stefka Kralchevska and Ms. Nikoleta Simeonova for carrying out a part of the solubilization measurements.

Appendix A: Principles of the Computational Procedure

The theoretical time dependence of the drop radius, $R(t)$, is given by eq 5.1. It is convenient to solve eq 5.1 with respect to the time t:

$$t = t_0 - \frac{1}{\alpha}R - \frac{\beta}{2\alpha^2}R^2 \qquad \text{(A1)}$$

In the experiment we record the diminishing of several oil drops for a given surfactant solution; see Figure 13. For each separate drop we obtain an experimental curve $R(t)$, which can be inverted as $t(R)$; see eq A1. The parameters α and β must be the same for all curves corresponding to a given solution, whereas t_0 is different for the different curves. In general, the experimental data points are

$$\{t_{ij}, R_{ij}\} \quad 1 \leq i \leq M \quad 1 \leq j \leq n_i \qquad \text{(A2)}$$

The subscript i numbers the experimental curves, whereas the subscript j numbers the data points belonging to a given curve; n_i is the number of data points at the ith

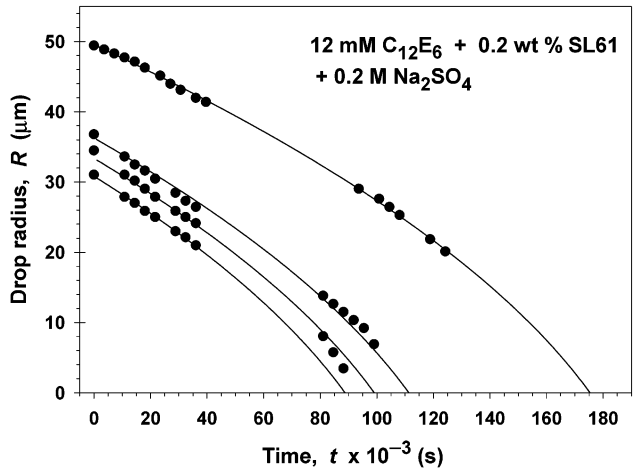

Figure 13. Time dependence, $R(t)$, of the radii of four diminishing triolein drops in a micellar solution of composition denoted in the figure (cell no. 2 used). The lines are the best fit of the data for the four drops, which are processed simultaneously as explained in Appendix A. The determined parameters α and β are given in Table 2, the last line.

curve and M is the number of experimental curves. In accordance with the least-squares method, we define the merit function

$$\Phi_i(t_{0i}, \alpha, \beta) = \sum_{j=1}^{n_i}\left[t_{ij} - \left(t_{0i} - \frac{1}{\alpha}R_{ij} - \frac{\beta}{2\alpha^2}{R_{ij}}^2\right)\right]^2 \quad \text{(A3)}$$

The best fit corresponds to a minimum of Φ_i with respect to t_{0i}. Correspondingly, from the condition for minimum, $\partial\Phi_i/\partial t_{0i} = 0$, we obtain

$$t_{0i}(\alpha, \beta) = \sum_{j=1}^{n_i} t_{ij} + \frac{1}{\alpha}\sum_{j=1}^{n_i} R_{ij} + \frac{\beta}{2\alpha^2}\sum_{j=1}^{n_i}{R_{ij}}^2 \quad \text{(A4)}$$

Next, to determine α and β we consider the total merit function, which accounts for the difference between theory and experiment for all curves:

$$\Phi(\alpha, \beta) = \sum_{i=1}^{M}\Phi_i(t_{0i}, \alpha, \beta) \quad \text{(A5)}$$

From eqs A3 and A4 we substitute Φ_i and t_{0i} into eq A5; thus, we obtain

$$\Phi(\alpha, \beta) = \sum_{i=1}^{M}\sum_{j=1}^{n_i}(A_{ij} + B_{ij}x + C_{ij}y)^2 \quad \text{(A6)}$$

where

$$x = 1/\alpha \quad y = \beta/(2\alpha^2) \quad \text{(A7)}$$

and A_{ij}, B_{ij}, and C_{ij} are coefficients independent of α and β:

$$A_{ij} = t_{ij} - \sum_{k=1}^{n_i} t_{ik} \qquad B_{ij} = R_{ij} - \sum_{k=1}^{n_i} R_{ik}$$

$$C_{ij} = {R_{ij}}^2 - \sum_{k=1}^{n_i}{R_{ik}}^2 \quad \text{(A8)}$$

The requirement for best fit, that is for minimum of Φ, yields

$$\frac{\partial\Phi}{\partial x} = 0 \quad \frac{\Phi}{\partial y} = 0 \quad \text{(A9)}$$

The substitution of eq A6 into eq A9 leads to a system of two linear equations for determining the variables x and y. This system (and our minimization problem) has a unique solution. From the determined values of x and y, which correspond to the best fit, we calculate the sought for parameters: $\alpha = 1/x$ and $\beta = 2\alpha^2 y$.

Appendix B: Solubilization under Diffusion Control

Consider an isolated oil drop whose radius R diminishes with time, t, due to solubilization in a micellar surfactant solution. Here, we assume that every collision of an empty micelle with the oil−water interface leads to the solubilization of a volume v_e of the oil. Thus, the empty micelle will be transformed into a full micelle at the surface of the oil drop. Further, we assume steady-state diffusion. Then, the concentration of the empty micelles, $c_1(r)$, satisfies the equation of the stationary diffusion

$$\frac{\mathrm{d}}{\mathrm{d}r}\left(r^2\frac{\mathrm{d}c_1}{\mathrm{d}r}\right) = 0 \quad r \geq R \quad \text{(B1)}$$

along with the boundary conditions

$$c_1(r = R) = 0 \quad c_1(r \to \infty) = c_{10} \quad \text{(B2)}$$

where c_{10} is the bulk concentration of the empty micelles. From eqs B1 and B2 we obtain $c_1(r) = (1 - R/r)c_{10}$. The flux of empty micelles/unit area of the oil-drop surface is

$$Q_1 = D_1\left(\frac{\mathrm{d}c_1}{\mathrm{d}r}\right)_{r=R} = \frac{D_1 c_{10}}{R} \quad \text{(B3)}$$

where D_1 is the diffusivity of the empty micelles. The decrease in the volume of the oil drop is due to the oil taken by the micelles:

$$\frac{\mathrm{d}}{\mathrm{d}t}\left(\frac{4}{3}\pi R^3\right) = -v_e 4\pi R^2 Q_1 \quad \text{(B4)}$$

By substituting eq B3 into B4 and some transformations, one derives eq 3.2.

LA020367C